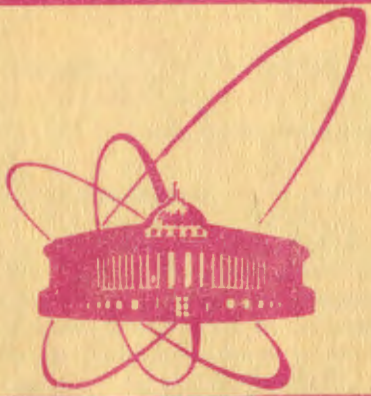

объединенный
институт
ядерных
исследований
дубна

E1-80-542

V.K.Birulev, V.P.Dzhordzhadze, V.I.Genchev,
T.S.Grigalashvili, B.N.Gus'kov, I.M.Ivanchenko,
V.D.Kekelidze, V.G.Krivokhizhin, V.V.Kukhtin,
M.F.Likhachev, I.Manno, A.V.Pose, H.-E.Rysek,
I.A.Savin, L.V.Silvestrov, V.E.Simonov,
G.G.Takhtamyshev, P.T.Todorov, G.Vesztergombi

A STUDY OF THE SEMILEPTONIC DECAYS OF NEUTRAL KAONS

Submitted to "Nuclear Physics"

1980

1. INTRODUCTION

The study of the semileptonic decays of K^0_L mesons $K^0_{e3} \to \pi^{\pm} e^{\mp} \nu_e$ and $K^0_{\mu 3} \to \pi^{\pm} \mu^{\mp} \nu_\mu$ can give valuable information both on the structure of the weak interaction (V-A theory, μ–e universality, $\Delta I = 1/2$ rule) and on several models and hypotheses of the strong interaction (current algebra, soft pion theorem, dispersion relations, etc.).

The most general matrix element for $K_{\ell 3}$ decays may be written as [1]:

$$M = \frac{G}{\sqrt{2}} \sin\theta_c \{ M_k f_s \bar{U}_\ell (1+\gamma_5) U_\nu + [f_+(k+q) + f_-(k-q)] \times$$
$$\times \bar{U}_\ell \gamma_\mu (1+\gamma_5) U_\nu + \frac{f_T}{2M_k} (k_\lambda q_\mu - k_\mu q_\lambda) \bar{U}_\ell \sigma_{\lambda\mu} (1+\gamma_5) U_\nu \}, \quad (1)$$

where θ_c is the Cabibbo angle, f_+ and f_- are the vector form factors, f_s and f_T are the scalar and tensor form factors, U_ℓ and U_ν are the lepton spinors, k and q are the kaon and pion four-momenta, M_k is the kaon mass.

Within the framework of the V-A theory $K_{\ell 3}$ decays can be described by two form factors $f_+(t)$ and $f_-(t)$, where t is the square of the four momentum transfer to the leptons. In this case the matrix element may be written as:

$$M \sim \bar{U}_\ell \gamma_\mu (1+\gamma_5) U_\nu [f_+(t)(k+q) + f_-(t)(k-q)]. \quad (2)$$

A decomposition of the vector part of the matrix element into terms corresponding to the 0^+ and 1^- spin-parity states of the dilepton system gives rise to two amplitudes which are related to the form factors f and f_+, where $f = f_+ + f_- t/(M_k^2 - m_\pi^2)$.

As a first approximation, the t dependence of the form factors is assumed to be linear:

$$f_+(t) = f_+(0)(1 + \lambda_+ t/m_\pi^2); \quad f(t) = f(0)(1 + \lambda_0 t/m_\pi^2). \quad (3)$$

The ratio of the form factors f_- to f_+ can also be approximated by a linear form:

$$\xi(t) = f_-(t)/f_+(t) = \xi(0) + \Lambda t/m_\pi^2. \quad (4)$$

Using eqs. (3) and (4), we obtain:

$$\xi(t) = \frac{M_k^2 - m_\pi^2}{m_\pi^2} \cdot \frac{\lambda_0 - \lambda_+}{1 + \lambda_+ t/m_\pi^2} . \qquad (5)$$

It is usually assumed that the form factors f_+ and f satisfy at most once subtracted dispersion relations. If the $f_+(t)$ and $f(t)$ amplitudes are unsubtracted, the dispersion integrals can be approximated by poles (zero-width resonances):

$$f_+(t) = f_+(0) \frac{M_*^2}{M_*^2 - t}; \quad f(t) = f(0) \frac{M_K^2}{M_K^2 - t}, \qquad (6)$$

where M_* and M_K are the resonance masses of the 1^- and 0^+ spin-parity states, respectively.

If the t^2 terms are neglected, the slope parameters λ_+ and λ_0 are related to M_* and M_K :

$$\lambda_+ = m_\pi^2/M_*^2; \quad \lambda_0 = m_\pi^2/M_K^2 . \qquad (7)$$

The Dalitz plot density of $K_{\ell 3}$ decays can be written as:

$$d^2N/dt\,dE_\nu = Af_+^2(t) + Bf_+(t)\,f(t) + Cf^2(t) , \qquad (8)$$

where E_ν is the neutrino energy in the kaon rest system, A,B,C are the known kinematical functions.

In this paper we present results of a study of 74000 K°_{e3} and 150000 $K^\circ_{\mu 3}$ decays. Preliminary results from this experiment have been reported elsewhere [2-5].

2. PERFORMANCE OF THE EXPERIMENT

The experiment was primarily designed to study the K°_L-K°_S transmission regeneration on hydrogen and deuterium. It was performed using a wire spark chamber spectrometer in a neutral beam of the Serpukhov 70 GeV proton synchrotron. The spectrometer detected all known types of K° decays: $K^\circ_{\pi 2} \to \pi^+\pi^-$; $K^\circ_{e3} \to \pi^\pm e^\mp \nu_e$; $K^\circ_{\mu 3} \to \pi^\pm \mu^\mp \nu_\mu$ and $K^\circ_{\pi 3} \to \pi^+\pi^-\pi^\circ$. A view of the experimental setup is shown in fig.1. The analysing magnet M had a field effective volume of 200x100x25 cm^3. Eighteen two-coordinate wire spark chambers were installed in front of and behind the magnet in groups of three each. Four scintillation counter hodoscopes FI, FII, GI, GII and three anticounters A, A_R, A_L were ised to trigger the spectrometer. The K°_{e3} and $K^\circ_{\mu 3}$ decays were identified with the help of the electron and muon detectors.

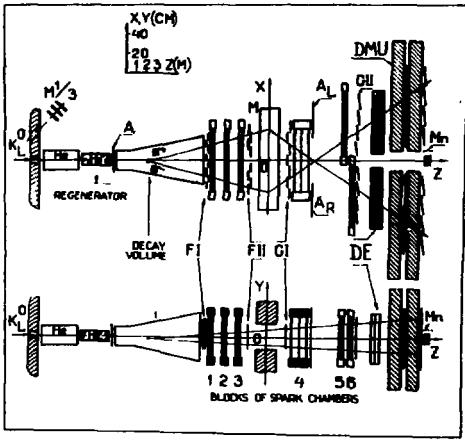

Fig.1. Experimental setup (top and side views). The notations are: M1/3. Side monitor; A, A_R, A_L. Anticounters; FI, FII, GI, GII. Scintillation counter hodoscopes; M. Analysing magnet; DE. Electron detector; DM. Muon detector; Mn. Neutron monitor.

The electron detector was composed of four "sandwich" type shower counters. Each counter had two identical units assembled from 10 scintillator plates with lead plates between them having an area of 55.5x30.0 cm^2. A light flash was recorded by two FEU-65 photomultipliers mounted on the top and at the bottom of each unit.

The muon detector consisted of two planes of scintillation counters and two sections of an iron filter 125 cm long each. The first plane of four scintillation counters was located between the filter sections and was connected in coincidence with the second one to decrease accidental counting rates of the detector. The second plane consisting of 10 20x64x2 cm^3 counters was used as a muon hodoscope.

The data were accumulated on magnetic tape by means of a BESM-3M computer. The event data included spark chamber coordinates, scintillation counter latches, shower counter pulse heights and information on beam monitoring. Details of the apparatus and of the K^0 beam have been given previously [6-10].

The geometric program reconstructed the events with two charged particles (V^0) which occurred in the decay volume.

The experimental has been carried out in two stages. The liquid hydrogen and liquid deuterium regenerators were used at the first and second stages, respectively. The data were handles independently at each stage. Later on we shall call them "experiment I" and "experiment II".

3. EVENT SELECTION

Event selection involved the following main steps: (a) preliminary identification of $K^{\circ}_{\mu 3}$ and K°_{e3} modes; (b) geometric and kinematic cuts; (c) final identification of the decay products.

If the extrapolation of one of the charged tracks hit the fired muon counter, the event was identified as a $K^{\circ}_{\mu 3}$ decay. The fiducial sizes of the muon counters were chosen taking into account muon scattering in iron.

If the extrapolation of the charged track hit the shower counter and the counter pulse height exceeded a certain level the event was classified as a K°_{e3} decay. The events which were candidates of $K^{\circ}_{\mu 3}$ and K°_{e3} decays were rewritten on separate magnetic tapes.

The geometric and kinematic cuts involved the following requirements:

(1) Z -coordinate of the decay vertex had to lie within the decay volume.

(2) X-and Y-coordinates of the tracks had to lie within the fiducial sizes of the corresponding elements: scintillation hodoscopes, spark chambers and shower counters.

(3) Other K° decay modes were rejected. The $K^{\circ}_{\pi 2}$ decay were rejected by the invariant mass of the $\pi^{+}\pi^{-}$ system; $0.508 \leq M_{\pi\pi} \leq .488$ (GeV/c) was required. The $K^{\circ}_{\pi 3}$ decays were rejected by the P'^{2}_{0} variables ; $P'^{2}_{0} \leq -4\,(\mathrm{MeV/c})^{2}$ was required.

(4) The reconstructed kaon momentum, $14 \leq P_{K} \leq 52$ (GeV/c) was required to be in accordance with the real K° momentum spectrum.

(5) The invariant masses of the $\pi\mu$ or πe systems has be smaller that the kaon mass.

(6) The difference between the center of mass neutrino momentum P^{*}_{ν} and the transverse momentum of the charged pair $P^{c}_{\perp}$ had to be positive: $\Delta P_{T} = P^{*}_{\nu} - P^{c}_{\perp} > 0$.

(7) The reconstructed events had to fall inside the Dalitz plot boundaries.

The boundary of electron identification was chosen more accurately at the final step. The following procedure was used. The amplitude spectrum of the shower counter pulses was obtained for 14 particle momentum intervals with $7 \leq P \leq 21$ (GeV/c). The electron peaks were seen quite well. They were fitted by the Gaussian distributions, and the center A_0 and the standard deviation σ were calculated for each momentum interval and for each shower counter. The depend

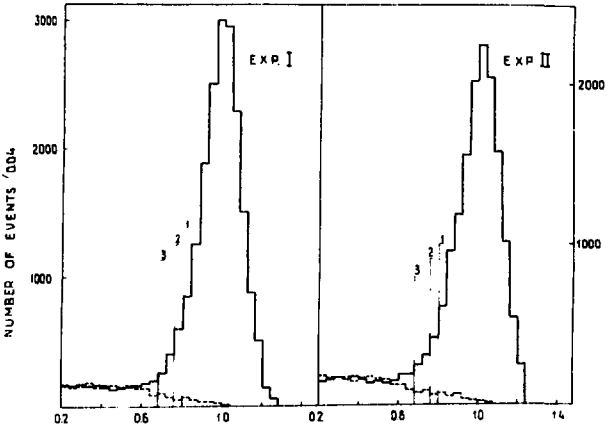

Fig.2. Distribution of the relative amplitude δA of pulses from the shower counters. Electron identification boundaries are denoted by figures 1,2,3.

of A_0 and σ on electron momentum P was fitted by the curves $A_0(P)$ and $\sigma(P)$, and then the "relative amplitude" δA was calculated: $\delta A = |A/A_0(P)| \times [\bar{\sigma}/\sigma(P)]$, where A is the amplitude observed, $\bar{\sigma}$ is the average standard deviation for all shower counters. The distribution of the δA amplitude is shown in fig.2. The lines marked 1,2,3 denote the boundaries of electron identification which were used in the K^0_{e3} decay analysis. They correspond to 2; 2.4; 3 standard deviations of the δA distribution. The event was identified as a K^0_{e3} decay if the δA value for one charged particle was larger than this boundary and δA for another charged particle was smaller than 0.5. The three different boundaries of electron identification were used to verify the stability of the results.

4. MONTE CARLO PROGRAM AND K^0_L MOMENTUM SPECTRUM

The information on the $K_{\ell 3}$ form factors was obtained by comparing the Dalitz plot density of experimental events and Monte-Carlo simulated events. In the Monte-Carlo program we took into account the errors in measuring track coordinates in the spark chambers, the spark chamber efficiency, multiple scattering of charged particles and electron bremsstrahlung

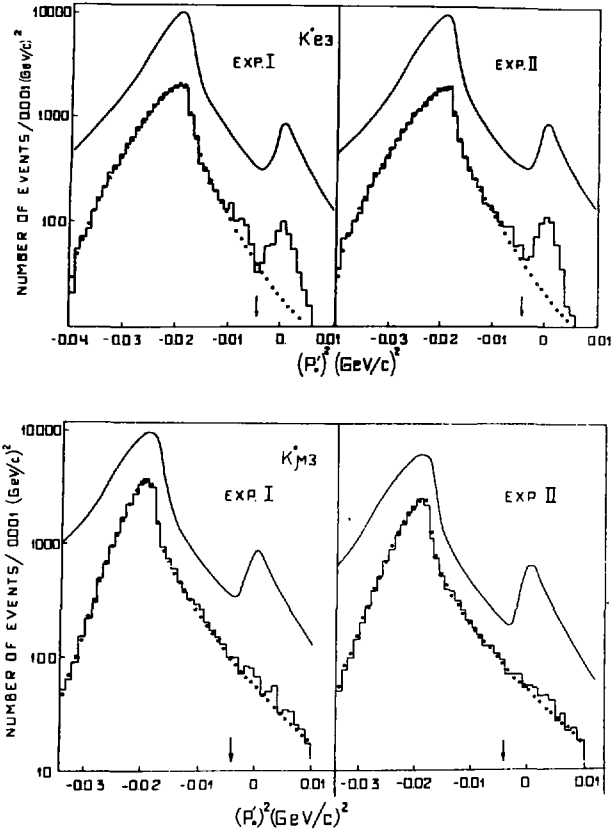

Fig.3. P'^2_0 distributions in the K°_{e3} and $K^\circ_{\mu 3}$ decays. The histograms are experimental events, the circles are Monte-Carlo simulations, the solid line denote all the decays detected in the experiment. The arrows indicate the cuts applied to the data.

in the setup matter, radiative corrections for the matrix element, K° elastic scattering in the liquid deuterium regenerator, and the real K°_L momentum spectrum.

The K°_{L} momentum spectrum was obtained from the selected $K^{\circ}_{\mu 3}$ and K°_{e3} decays independently. As for each event there exists a two-fold ambiguity in the calculation of the K°_{L} momentum, a statistical method of spectrum reconstruction was used [12]. The spectrum was reconstructed also from $K^{\circ}_{\pi 3}$ and $K^{\circ}_{\pi 2}$ decays. All results are in agreement.

The Monte-Carlo events were reconstructed by the same geometric program and they were processed by the same selection criteria as the true experimental events.

Two of the most sensitive tests for Monte-Carlo simulation were provided by the distribution of variables P'^{2}_{0} and ΔP_{T} These distributions for the experimental and simulated events are shown in figs. 3 and 4. The agreement between both kinds of the data confirms that all experimental conditions were taken into account correctly in the Monte-Carlo program.

5. BACKGROUND

The detection of all K° decay modes permits one to study in detail the background and systematic effects in this experiment. We have found that abour 5% of all events are not attributed to the known K° decay modes (the so-called "non-identified V°-events"). They are mainly due to the inelastic interaction of beam particles with the matter of the regenerator, anticounter and decay volume and to the mistakes by the geometric reconstruction of V° samples. These events can be the sources of the background if one of two particles is identified incorrectly as an electron or a muon.

In fig.2 the dotted line shows the amplitude pulse spectrum from the electron detector when it is crossed by pions selected from $K^{\circ}_{\mu 3}$ decays. The events in that part of the spectrum which lies on the right side of the electron identification boundary initiates "false" K°_{e3} decays. The contamination of this background relative to all K°_{e3} decays was found to be $(2.0\pm0.5)\%$ in experiment I and $(1.5\pm0.5)\%$ in experiment II. These estimates were checked by the number of events in which both particles were identified as electrons. Both estimates are in agreement.

The following procedure was used to subtract the background. The non-identified events were selected and rewritten on separate magnetic tapes. The mass of one particle was assigned as the electron mass, and these events were processed by all selection criteria for the K°_{e3} decays. For the remaining events the Dalitz plot was constructed which was subtracted from the Dalitz plot for all K°_{e3} events with the corresponding normalization coefficient.

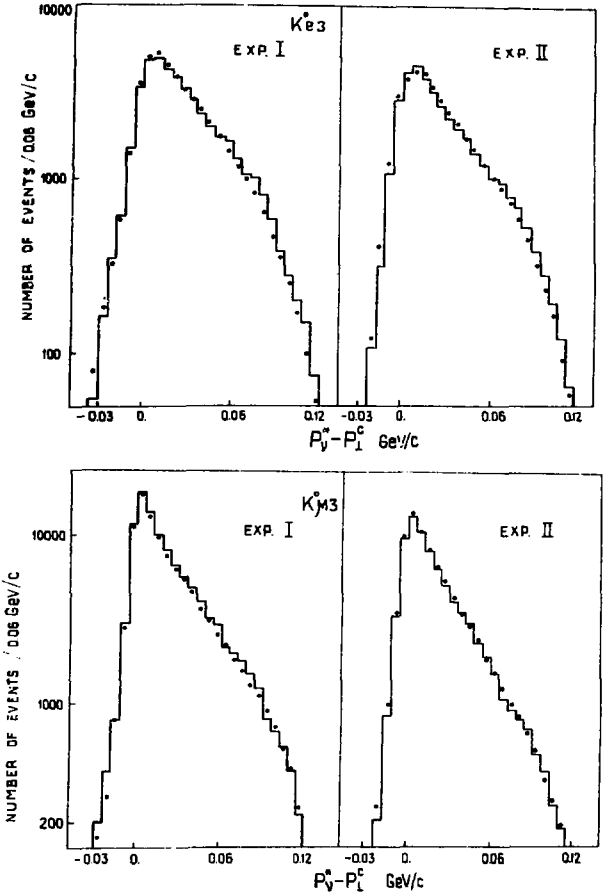

Fig.4. $\Delta P_T = P^*_\nu - P_\perp$ distribution in the K^0_{e3} and $K^0_{\mu 3}$ decays. The histograms are experimental events, the circles are Monte-Carlo simulations.

In the case of $K^0_{\mu 3}$ decays the source of the background is decays in flight (we assume that at least one charged particle in the non-identified events is pion). This back-

ground was estimated by two methods: (a) from $\mu+\mu$ events when two particles were identified as muons and (b) from Monte-Carlo calculation. Both estimates were in agreement, and the background contamination relative to all $K^{\circ}_{\mu 3}$ decays was found to be equal to (3.0±1.0)% in the experiment I and to (3.2±1.1)% in the experiment II. The procedure of background subtraction was similar to that used for K°_{e3} decays.

6. ANALYSIS OF K°_{e3} DECAYS

In studies of semileptonic K°_{L} decays the validity of V-A theory is usually supposed, and the matrix element is parametrized as in (2). Then the information on the f_+ and f_- form factors is used to investigate the contribution of the scalar and tensor form factors to the general matrix element (1).

The terms involving the form factor f_- is proportional to the lepton mass and can be safely neglected in the case of K°_{e3} decays. Then the Dalitz plot density takes the simple form

$$d^2N/dt\,dE_{\nu} = A f_+^2(t) .$$

The total number of selected K°_{e3} decays was equal to 48000 true and 75000 simulated events in the experiment I and to 26000 true and 60000 simulated events in the experiment II.

The dependence of the form factor f_+ on t was analysed by two methods.

(1) In a model-independent analysis the average values of $f_+(t)$ were determined in 10 intervals of t from 0 to 0.10 $(GeV/c)^2$. Since for each event there exists a two-fold ambiguity in the calculation of t, only those events were selected where both solutions t_1 and t_2 lay in the same $10^2(MeV/c)^4$ bin (the so-called "diagonal events"). The acceptance efficiency for these events in per cent as a function of Dalitz plot position is shown in fig.5. The values of the form factor f_+ obtained in such a way are shown in fig.6. The results of the linear fit of the data is presented in this figure as well.

(2) In a model-dependent analysis the linear expansion $f_+(t)$ (eq. 3) was assumed. We used both values of t and constructed the 3-simensional Dalitz plot $t_1 \times t_2 \times E_{\nu}$ with bin sizes of 10 $(MeV/c)^2 \times 10$ $(MeV/c)^2 \times 20$ MeV. The bins which lay near the Dalitz plot boundaries were combined so that the number of events in each bin exceeded 20. The parameter λ_+^e was determined as a free parameter by fitting this distribution to

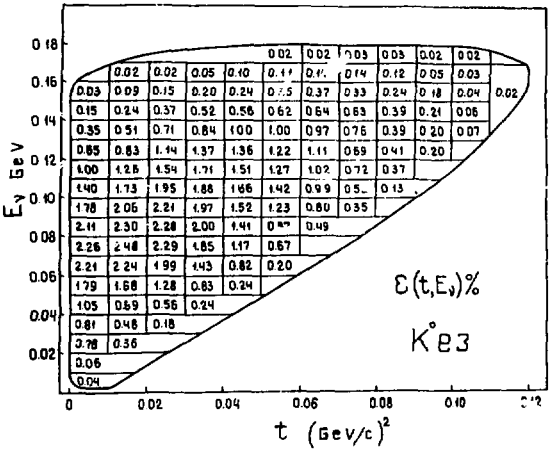

Fig.5. Acceptance efficiency, $\epsilon(t,E_\nu)$, of the K°_{e3} decays in per cent as a function of the Dalitz plot position.

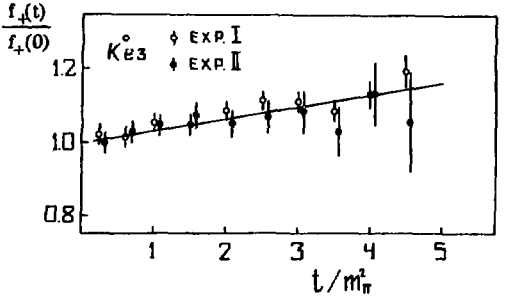

Fig.6. Values of the form factor $f_+(t)$ obtained in the model-independent analysis of the K_{e3} decays. The solid line is the result of linear fit.

the Monter-Carlo simulation calculated for $\lambda^e_+=0$. The same analysis was made for diagonal events as well.

The influence was studied of the systematic effects on the uncertainty in the slope parameter in the case of the linear fit. A more complete verification of the self-consistency of our data is a comparison between the results of experiment I and II. These experiments differ from one another in

Table 1

Contribution of the systematic effects to the $\Delta\lambda_+^e$ uncertainty for K^0_{e3} decays

Sources of effects	$\Delta\lambda_+^e$
Different boundaries of electron identification ($2\sigma \leq A \leq 3\sigma$)	0.001
Different cuts of the minimal number of events in one bin (20-30)	0.001
Uncertainty in background per cent (1.5-2.5)%	0.001
Uncertainty in the fraction of elastic scattered in the deuterium regenerator (1.5-3.0)%	0.001
Difference between results of experiments I and II and their weighted average	0.0017
Total uncertainty	0.0026

Table 2

Form factor slope λ_+^e in K^0_{e3} decays

Analysis method	№ of experiment	Statistics	λ_+^e	$\frac{\chi^2}{d.f.}$
Model-independent	I+II	21 000	0.032 ± 0.004	0.4
Linear expansion (diagonal events)	I+II	21 000	0.026 ± 0.005	1.4
Linear expansion (all events)	I	48 000	0.0320 ± 0.0042	1.24
	II	26 000	0.0286 ± 0.0049	1.29
	I+II	74 000	0.0306 ± 0.0034	1.26

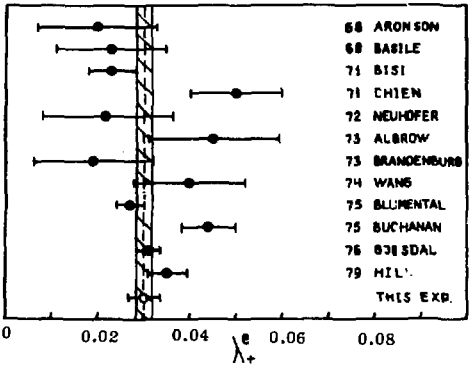

Fig.7. Values of λ_+^e obtained in the K°_{e3} experiments. The hatched area is the world-average value of λ_+^e with its error. The references are: Aronson [13], Basile [14], Bisi [15], Chien [16], Neuhofer [17], Albrow [18], Brandenburg [19], Wang [20], Blumental [21], Buchanan [22], Gjesdal [23], Hill [24].

the following features: (a) different geometric position of the electron detector, (b) different high voltage on its photomultipliers, (c) different position of the accelerator target, (d) different regenerators. The contribution of other systematic effects to the uncertainty $\Delta\lambda_+^e$ is given in table 1.

Table 2 gives the values of λ_+^e obtained by different methods. The average value of the slope in experiments I and II is equal to $\lambda_+^e = 0.0306 \pm 0.0034$.

A comparison between the values of λ_+^e obtained from the K°_{e3} experiments shows a good agreement of our result with the world average value (fig.7).

7. ANALYSIS OF $K^\circ_{\mu 3}$ DECAYS

The total numbers of selected $K^\circ_{\mu 3}$ decays were equal to 82000 true and 110000 simulated events in the experiment I and to 68000 true and 220000 simulated events in the experiment II. The analysis was made by the same way as for K°_{e3} decays. In the case of $K^\circ_{\mu 3}$ decays the Dalitz plot density is described by expression (8). The acceptance efficiency for diagonal events as a function of Dalitz plot position is shown in fig.8.

In a model-independent analysis the average values of $f_+(t)$ and $f(t)$ were determined in 10 intervals of t from 0.01 to 0.11 $(GeV/c)^2$. The values of the form factors f_+ and f and the linear fit results are shown in fig.9. The slopes λ_+^μ and λ_0 obtained both in the model-independent and in the linear-model analysis are given in table 3. In the latter case

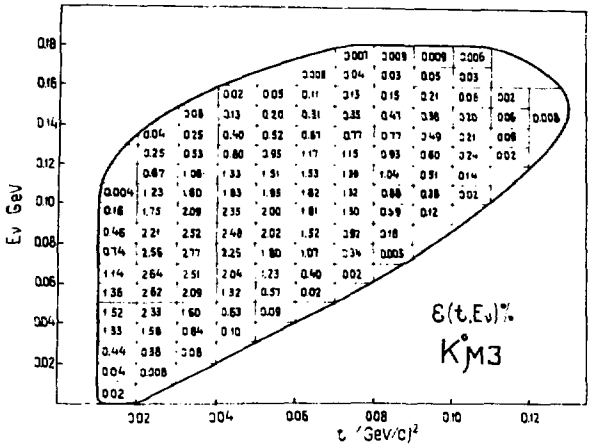

Fig.8. Acceptance efficiency, $\epsilon(t, E_\nu)$, of the $K^\circ_{\mu 3}$ decays in per cents as a function of the Dalitz plot position.

the errors include the systematic effects. The contribution of these effects to the uncertainty $\Delta\lambda^\mu_+$ and $\Delta\lambda_0$ are given in table 4. The average values of the slopes in the experiments I and II are equal to: $\lambda^\mu_+ = 0.0427 \pm 0.0044$; $\lambda_0 = 0.0341 \pm 0.0067$.

The results obtained by the different methods of analysis agree with each other and with our preliminary results within the errors [2,3]. The ambiguity of the solutions for the slope parameters observed at the preliminary stage was removed due to a careful calculation of the systematic effects. The investigation of χ^2 as a function of λ^μ_+ and λ_0 shows the existence of one minimum which corresponds to the presented values of these parameters.

8. DISCUSSION OF THE RESULTS

8.1. Scalar and Tensor Contribution

Both K°_{e3} and $K^\circ_{\mu 3}$ modes have been used to investigate the contribution of other terms to the decay matrix element except those of a pure vector nature. We assumed a linear parametrization of the vector form factor $f_+(t)$ and constant scalar and tensor form factors f_S and f_T. For the K°_{e3} decay mode we

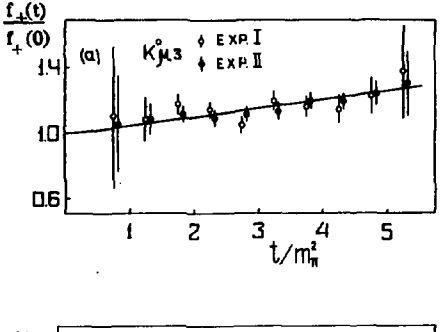

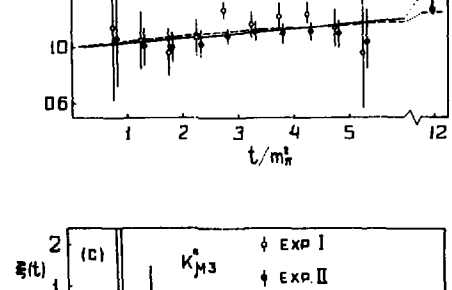

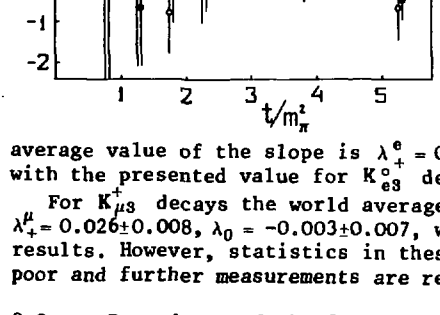

Fig.9. (a) Values of the form factor $f_+(t)$ obtained in the model independent analysis of the $K^0_{\mu 3}$ decays. The solid line is the result of linear fit. (b) The same for the form factor $f(t)$. ■ - Callan-Treiman point, □ - result of linear extrapolation of our data. The dashed line is the result of calculation by the Barut's model [27]. (c) Data of $\xi(t)$ model-independent analysis.

found $|f_S/f_+| < 0.07$ and $|f_T/f_+| < 0.34$ at a 68% confidence level. For the $K^0_{\mu 3}$ decay mode we found $|f_T/f_+| = 0.12 \pm 0.12$ or $|f_T/f_+| < 0.24$ at a 68% confidence level.

8.2. $\Delta I = 1/2$ Rule

If the $\Delta I = 1/2$ rule is valid in semileptonic kaon decays, then the form factors in neutral and charged kaon decays should be described by the same parameters. For K^+_{e3} decays the world average value of the slope is $\lambda^e_+ = 0.0285 \pm 0.0043$ [25]. It agrees with the presented value for K^0_{e3} decays: $\lambda^e_+ = 0.0306 \pm 0.0034$.

For $K^+_{\mu 3}$ decays the world averages of the slopes are $\lambda^\mu_+ = 0.026 \pm 0.008$, $\lambda_0 = -0.003 \pm 0.007$, which disagree with our results. However, statistics in these experiments is rather poor and further measurements are required.

8.3. t-Dependence of the Form Factor f_+

The best known theoretical model which related to the form factor f_+ is the Callan-Treiman (CT) relation [26]. Its

Table 3

Form factor slopes λ_+^μ and λ_0 in $K^0_{\mu 3}$ decays

Analysis method	HPD of experiment	Statistics	λ_+^μ	λ_0	$\frac{\chi^2}{d.f.}$
Model-independent	I+II	49 000	0.045±0.007	0.032±0.006	0.4
Linear expansion (diagonal events)	I+II	49 000	0.036±0.007	0.034±0.008	1.24
Linear expansion (all events)	I	82 000	0.0429±0.0061	0.0337±0.0094	1.28
	II	68 000	0.0424±0.0055	0.0345±0.0082	1.02
	I+II	150 000	0.0427±0.0044	0.0341±0.0067	1.15

The correlation between λ_0 and λ_+ is equal to $d\lambda_0/d\lambda_+ = -1.5$

Table 4

Contribution of systematic effects to the $\Delta\lambda_+^\mu$ and $\Delta\lambda_0$ uncertainty for $K^0_{\mu 3}$ decays

Sources of effects	$\Delta\lambda_+^\mu$	$\Delta\lambda_0$
Different cuts of the minimal number of events in one bin (20-30)	0.001	0.002
Uncertainty in background per cent (2-4)%	0.0006	0.0014
Uncertainty in the fraction of elastic scattered K^0 in the deuterium regenerator (1.5-3.0)%	0.001	0.001
Difference between results of experiments I and II and their weighted average	0.0003	0.0004
Total uncertainty	0.0016	0.0026

derivation is based on current algebra and the assumption of PCAC. The CT relation determines the value of f at the unphysical point $t = M_K^2 - m_\pi^2$:

$$f(M_K^2 - m_\pi^2) = f_+ (M_K^2 - m_\pi^2) + f_-(M_K^2 - m_\pi^2) = f_K/f_\pi = 1.27 \pm 0.03,$$

where f_K and f_π are the $K_{\ell 2}$ and $\pi_{\ell 2}$ decay constants.

If we assume a linear t-dependence of f and substitute expression (3), we found $\lambda_0 = 0.023 \pm 0.003$.

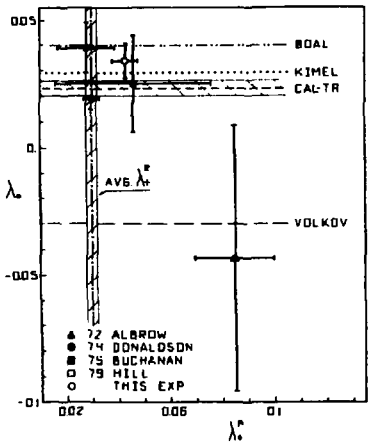

Fig.10. Values of λ'_+ and λ_0 obtained in the $K^0_{\mu 3}$ experiments with high enough statistics. The horizontal lines are the results of calculation of λ_0 in the different models. The references are: Albrow [28], Donaldson [29], Buchanan [22], Hill [30], Boal [31], Kimel [32], Volkov [33]. The vertical hatched area is the world-average value of λ_+^e with its error.

Figure 9(b) shows the CT point and the corresponding value of f obtained by a linear extrapolation of our data. Figure 10 gives the parameters λ'^{μ}_{+} and λ_0 determined in this experiment and in some recent experiments with high enough statistics. The horizontal lines show the λ_0 values calculated in different theoretical models. Boal founded his model on hard meson techniques [31]. Kimel applied current algebra and the assumption of form factor linearity [32]. Volkov et al. used a one-loop approximation within the framework of chiral quantum field theory [33]. The hatched area shows the CT prediction with its error. Our data agree with the Boal's and Kimel's calculation and slightly worse the CT prediction.

In fig.9(b) the dashed line shows the result of calculation by the model using the techniques of the relativistic wave functions (Barut) [27]. As is shows, this model is not contradiction to our data and agrees with the CT relation.

8.4. Ratio of Form Factors $\xi(t)$

A general theoretical prediction consist in the fact that $\xi(0)$ must be proportional to the first-order of breaking of the SU(3) symmetry [1,34] : $\xi(0) \approx -0.2$. In fig.9(c) the results of the model-independent analysis of $\xi(t)$ are shown. We have found the following values of $\xi(0)$ and Λ using expressions (4), (5) and λ'^{μ}_{+}, λ_0 obtained in the linear-model analysis: $\xi(0) = -0.10 \pm 0.09$; $\Lambda = 0.03 \pm 0.003$.

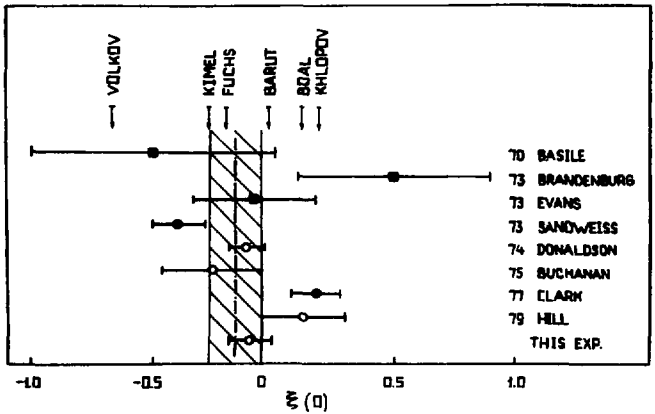

Fig.11. Values of $\xi(0)$ determined by different methods: ■ - from the $\Gamma(K^0_{\mu 3})/\Gamma(K^0_{e3})$ ratio, ● - from the measurement of muon polarization, o - from the Dalitz plot analysis. The references are: Basile [35], Brandenburg [19], Evans [36], Sandweiss [37], Clark [38], Donaldson [29], Buchanan [22], Hill [30], Volkov [33], Kimel [32], Fuchs [39], Barut [27], Boal [31], Khlopov [40].

Fugure 11 summarizes the values of $\xi(0)$ obtained in the experiments that have been performed by different methods. The hatched area shows the world-average value and its error. The arrows indicate the $\xi(0)$ value calculated in various models. Fuchs used current algebra and one-subtracted dispersion relations [39]. Khlopov carried out the calculation taking into account heavy quarks. The remaining models were described in section 8.3.

Our data are in agreement with the world-average value of $\xi(0)$ and with the simple quark model prediction. From concrete models they agree with the one-subtracted dispersion relations (Fuchs) and with the relativistic wave function model (Barut).

8.5. Verification of Pole Models

If the strong interaction between the kaon and the pion is assumed to dominate in the intermediate state, then in pole expressions (6) M_* and M_κ are the masses of $K^*(892,1^-)$

and $\kappa(1100\text{–}1400, 0^+)$ resonances (the existence of κ is indicated by some data). In the case of K^0_{e3} decays we fitted our data by the pole expression (6) and found the resonances mass $M_* = (835\pm40)$ MeV/c^2. This is in rough agreement with the K* mass. The value of M_* calculated using the approximate formulae (7) coincides with that value within some per cent.

In the case of $K^0_{\mu 3}$ decays we used the expression (7) and found the masses $M_* = (680\pm40)$ MeV/c^2 and $M_\kappa = (760\pm70)$ MeV/c^2. These data disagree with the masses of the K* and κ resonances. This means that the form factors in $K^0_{\mu 3}$ decays must be described by more complicated expressions than simple pole models: either by one-subtracted dispersion relations as supposed in the Fuchs's model or the sum of pole and dipole terms as assumed in the Barut's model.

8.6. t -Dependence of the Form Factor f_+ and the Problem of μ–e Universality

The vertical hatched area in fig.10 is the world-average value of the slope parameter λ_+^e from K^0_{e3} decays with its error (see fig.7 as well). As can be seen the value of λ_+^μ obtained in this experiment in the $K^0_{\mu 3}$ decays differs by about two standard errors from this value of λ_+^e and from the value that we obtained in the K^0_{e3} decays (see section 6). Quantitatively, in our experiment the difference between the form factor slopes in the K^0_{e3} and $K^0_{\mu 3}$ decays is equal to: $\lambda_+^\mu - \lambda_+^e = 0.012\pm0.005$. This can be some indication of the violation of μ–e universality in the semileptonic decay of K°-mesons.

In this connection we should like to note the following. In many experiments in which the parameters of muon and electron interactions are measured immediately, these parameters are also distinguished by about 2-3 standard errors: for instance, the measurement of muonic atoms [41], elastic muon and electron scattering on hydrogen[42], the ratio of $\Gamma(\pi\to e\nu)/\Gamma(\pi\to\mu\nu)$ and verification of the Goldberger-Treiman relation [43]. In some kaon decay experiments there are also indications that the value of λ_+^μ in $K^0_{\mu 3}$ decays is somewhat larger than the same value of λ_+^e in K^0_{e3} decays [44].

In the theoretical aspect the discovery of τ -lepton and the possibility of existence of other heavy leptons have led to the revision of the μ–e universality problem. Now it is not considered as the common requirement of theory. Various models are siggested to explain the μ–e universality violation. They involve: the new type of interaction in which elect-

rons and muons participate in the non-symmetric manner [45], mixing with heavy leptons [46], symmetry groups with right-handed currents [47], etc.

Thus, data on the non-universality of electron and muon are accumulated both in theory and in experiment. Further measurements are required towards this direction.

9. CONCLUSIONS

I. The results of analysis of both K^0_{e3} and $K^0_{\mu 3}$ decay modes allow one to draw the following conclusions.

(1) The matrix element for $K_{\ell 3}$ decays is compatible with the absence of scalar and tensor contributions to the strangeness-changing hadron current.

(2) No significant deviation from the linear model has been observed in the behaviour of the form factors $f_+(t)$ and $f(t)$ which describe the vector contribution to the decay matrix element. However, our data do not contradict the small non-linearity that is supposed in the model [27].

II. For K^0_{e3} decays the obtained slope λ^e_+ of the form factor $f^e_+(t)$ is in good agreement with the results of recent experiments and with the world-average value. It is also agress with the value of λ^e_+ obtained in K^+_{e3} decays. We can draw the following conclusion for this decay mode.

(1) The $\Delta I=1/2$ rule is valid within the accuracy of the experimental data.

(2) The form factor $f^e_+(t)$ can be described by the unsubtracted dispersion relations with the dominance of the $K^*(892)$ pole.

III. For $K^0_{\mu 3}$ decays a fairly large discrepancy is observed between the results of studying the form factors so that no single-values conclusion can be made for all experiment*. The results of the present experiment allow the following conclusions to be drawn.

(1) The soft pion theorems and SU(2)xSU(2) algebra are a good approach to the description of $K^0_{\mu 3}$ decays. There is an attractive model based on the relativistic wave function technique which describes electromagnetic and weak form factors in the same manner [27].

---

*We would like to note that this discrepancy relates to the linear model analysis. If one assumes a small non-linearity in the form factor behaviour, then the best agreement may be reached between experiments.

(2) The form factors $f_+(t)$ and $f(t)$ can be described by the dispersion relations with one or more subtraction.

(3) The form factor ratio $\xi(t)$ is in accord with the simple quark model of SU(3) breaking.

(4) The comparison of the form factors in K^0_{e3} and $K^0_{\mu 3}$ decays indicates the possibility of μ-e universality violation in these processes.

APPENDIX. $K_{\ell 3}$ Decays and Quark Masses

In the last years the number of papers have been published in which the light quark masses m_u, m_d, m_s and their ratio are calculated. The obtained results are mainly divided into two groups.

(1) The calculation founded on baryon and meson mass spectra and baryon magnetic moments [34,48] gives: $m_u \approx m_d \approx$ $\approx$(313-336) MeV, $m_s \approx$ (530-560) MeV, $m_s/m_d \approx 1.6$. The quarks considered in these models were called "constituent".

(2) The calculation founded on the expressions of currents or their divergences gives the quark masses [49,50]: $m_u \approx$ $\approx$(1.8-5.6) MeV, $m_d \sim$ (4.3-14.6) MeV, $m_s \approx$ (112-378) MeV, $(m_u+m_d)/(m_d+m_s) \approx 0.04$-$0.08$. In this case the quarks were called "current".

Recently it has been shown that from the calculation founded on the σ-model the mass ratio can be obtained both for constituent and for current quarks [51]. A similar situation takes place in $K_{\ell 3}$ decays.

As shown in section 8.4, $\xi(0)$ must be proportional to the first order of breaking of the SU(3) symmetry. The breaking parameter is equal to: [34]: $C = \sqrt{2}(\hat{m}-m_s)/(m_s+2\hat{m})$ (here $\hat{m} = (m_u+m_d)/2$).). From our value of $\xi(0)$ we have found: $m_s/\hat{m} = 1.23 \pm 0.22$. This is close to the constituent quark mass ratio.

On the other hand, the following expressions were obtained from current algebra and PCAC [52,53]:

$$f(M^2_{K^0}) = \frac{M^2_{K^0}}{M^2_{K^0} - m^2_{\pi^+}} \cdot \frac{f_K}{f_\pi}\left(1 - \frac{m_u + m_d}{m_d + m_s}\right). \qquad (10)$$

$$\xi \approx \frac{m^2_\pi/M^2_K - (m_u+m_d)/(m_d+m_s)}{m^2_\pi/M^2_K + (m_u+m_d)/(m_d+m_s)}, \qquad (11)$$

We have found from these expressions and from our values of $f(M_{K^0}^2)$ and $\xi(0)$:

$(m_u + m_d)/(m_d + m_s) = 0.04 \pm 0.09$ (from exp.10)

$(m_u + m_d)/(m_d + m_s) = 0.09$ (from exp.11).

This agrees with the mass ratio of the current quarks.

REFERENCES

1. Chounet L.M., Gaillard J.M., Gaillard M.K. Phys.Rep., 1972, 4C, p.201.
2. Albrecht K.F. et al. Phys.Lett., 1974, 48B, p.393.
3. Genchev V.I. et al. JINR, P1-9032, Dubna, 1975.
4. Birulev V.K. et al. JINR, P1-6164, Dubna, 1971; Yad.Fiz., 1976, 24, p.340.
5. Birulev V.K. et al. Yad.Fiz., 1979, 29, p.1515.
6. Basiladze S.G. et al. JINR, P1-5361, Dubna, 1970.
7. Vovenko A.S. et al. JINR, P1-7460, Dubna, 1973.
8. Grigalashvili T.S. et al. JINR, P3-5324, Dubna, 1970.
9. Birulev V.K. et al. JINR, 1-7307, Dubna, 1973.
10. Albrecht K.F. et al. JINR, 1-7305, Dubna, 1973.
11. Vesztergombi G. et al. Yad.Fiz., 1974, 20, p.371.
12. Takhtamyshev G.G. JINR, 2543, Dubna, 1966.
13. Aronson S.H. et al. Phys.Rev.Lett., 1968, 20, p.287.
14. Basile P. et al. Phys.Lett., 1968, 26B, p.542.
15. Bisi V. et al. Phys.Lett., 1971, 36B, p.533.
16. Chien C.-Y. et al. Phys.Lett., 1971, 35B, p.261.
17. Neuhofer G. et al. Phys.Lett., 1972, 41B, p.642.
18. Albrow M.G. et al. Nucl.Phys., 1973, B58, p.22.
19. Brandenburg G.W. et al. Phys.Rev., 1973, D8, p.1978.
20. Wang L. et al. Phys.Rev., 1974, D9, p.540.
21. Blumental R. et al. Phys.Rev.Lett., 1975, 34, p.164.
22. Buchanan C.D. et al. Phys.Rev., 1975, D11, p.457.
23. Gjesdal G. et al. Nucl.Phys., 1976, B109, p.118.
24. Hill D.G. et al. Phys.Lett., 1978, 73B, p.483.
25. Bricman C. et al. Rev.of Part.Prop., Geneva, 1980.
26. Callan C.G., Treiman S.B. Phys.Rev.Lett., 1966, 16,p.153; Dashen R., Weinstein M. Phys.Rev.Lett., 1969, 22, p.1337.
27. Barut A.O., Wilson R. Phys.Rev., 1979, D19, p.260.
28. Albrow M.G. et al. Nucl.Phys., 1972, B44, p.1.
29. Donaldson G. et al. Phys.Rev., 1974, D9, p.2999.
30. Hill D.G. et al. Nucl.Phys., 1979, B153, p.39.
31. Boal D.H., Graham R.H. Phys.Rev., 1977, D15, p.1878.
32. Kimel I. Lett. Nuovo Cim., 1976, 15, p.619.
33. Volkov M.K. et al. JINR, P2-9884, Dubna, 1976.

34. Gunion J.F. et al. Nucl.Phys., 1977, B123, p.445;
Lipkin H.J. Phys.Lett., 1978, 74B, p.399.
35. Basile P. et al. Phys.Rev., 1970, D2, p.78.
36. Evans G.R. et al. Phys.Rev., 1973, D7, p.36.
37. Sandweiss J. et al. Phys.Rev.Lett., 1973, 30, p.1002.
38. Clark A.R. et al. Phys.Rev., 1977, D15, p.553.
39. Fuchs N.H. Phys. Rev., 1968, 172, p.1532.
40. Khlopov M.Ju. Yad.Fiz., 1978, 28, p.1134.
41. Dixit M.S. et al. Phys.Rev.Lett., 1971, 27, p.878.
42. Walter H.K. et al. Phys.Lett., 1972, 40B, p.197.
42. Kostoulas I. et al. Phys.Rev.Lett., 1974, 32, p.489.
43. Ballin D., Dombey N. Phys.Lett., 1976, 64B, p.304.
44. Dally E. et al. Phys.Lett., 1972, 41B, p.647; Haidt D.
et al. Phys.Rev., 1971, D3, p.10.
45. Veltman M. Phys.Lett., 1977, 70B, p.253.
46. Lipmanov E.M., Michailov N.V. Yad.Fiz., 1979, 29, p.1091.
47. Fritzch H. et al. Phys.Lett., 1976, 59B, p.256;
Volkov G.G. et al. Yad.Fiz., 1979, 29, p.1276.
48. De Rujula A. et al. Phys.Rev., 1975, D12, p.147.
49. Gell-Mann H. et al. Phys.Rev., 1968, 175, p.2195.
50. Langacker P., Pagels H. Phys.Rev., 1979, D19, p.2070;
Pagels H., Stokar S. The Rockfeller Univ. Preprint.
COO-2232, B-194, 1980.
51. Socolovsky M. Phys.Lett., 1980, 90B, p.116.
52. Dominguez C.A. Phys.Lett., 1979, 86B, p.171.
53. Kaneco T. Progr.Theor.Phys., 1969, 42, p.428.

Received by Publishing Department
on July 30 1980.